Available online at http://scik.org
J. Math. Comput. Sci. 11 (2021), No. 3, 3331-3346
https://doi.org/10.28919/jmcs/5346
ISSN: 1927-5307

GALERKIN FINITE ELEMENT MODELING OF THERMOHALINE FLUID IN AN INCLINED CAVITY

RADHIKA MENON[1], DEEPA JOSHI[1], SANDHYA KADAM[1,*], DEEPAK SINGH[2]

[1]Dr. D. Y. Patil Institute of Technology, Pimpri, Pune-18, India

[2]NITTR, Bhopal, MP, India

Abstract. The knowledge of the behavior of thermo-solute in a confined space shall open up many application areas in control process. Flow analysis of a Thermohaline fluid inside a square cavity inclined at angle 'ϕ_0' with X-axis under steady state conditions has been investigated has been investigated.. The equations are modified with respect to rotational symmetry of groups. The resulting partial differential equations are modelled using Finite Element Technique. Also we have established a set of shape functions applicable to fourth order partial differential equations. Shape functions and the corresponding surfaces are characterized with respect to its properties. Algorithm has been developed for the computation. This model can be extended to analysis of largescale double diffusive convection subjected to complex boundaries.

Keywords: partial differential equation; numerical method; flow cavity; thermohaline fluid.

2010 AMS Subject Classification: 35G05, 65M06.

1. INTRODUCTION

Mathematical models for Benard convection with respect to boundary layer, temporal and steady state behavior has been investigated and analysed since 1975. Study of Cavity flow plays a vital role in several engineering applications extending to automobiles, aircrafts to riverbed

*Corresponding author

E-mail address: sandhyakadam08@gmail.email

Received December 23, 2020

channels and large scale flows. Gill [1] studied the cavity flow in a two dimensional rectangular cavity with vertical walls maintained at different temperature with huge difference in temperature. Garandet [2] proposed an analytic solution to the problem of buoyancy driven flow via two-dimensional shallow cavity with a transverse magnetic field. The resulting flow has been studied by means of series expansion. Ozoe and Okkado [3] investigated flow inside and over a square cavity with vertical walls at constant temperature, horizontal walls being insulated to three dimensional situations. They found that a field horizontal but parallel to the heated surface was observed to be least effective in suppressing the circulation of flow.

As a continuation of this work Vasseur [4] has studied the effect of transverse magnetic field on the natural convection in an inclined fluid layer using 2-D Navier-Stokes equation including Lorentz's force terms. Thermal conditions are taken to be cooling through opposite walls. Resulting equations are linearized through parallel flow approximations and analytical solutions are obtained for a shallow layer. These results are verified numerically using Finite difference approach.

In the recent studies,it is observed that thermohaline circulation from equator to poles plays a major role in prediction of climate changes Veronis type of Thermal convective flows between differentially heated horizontal/vertical plates has been studied by Banerjee etal [5] . Whitehead [6] studied abrupt transitions in a thremohaline loop through a laboratory model for Stommel type of situations. A distinct abruptive transition were observed in case the cavity experiments even when no measurable hysteresis was found . Menon [7],[8] investigated the flow field characteristics and stability analysis of thermohaline fluids under sinusoidal heating which simulates the solar heating in most of naturally occurring phenomenas.

The flow field characterization of thermohaline fluids inside a cavity gives insight into various hydrodynamic problems related to fluid flow analysis across a coastal regions estuaries straits and Shelves. More over finite element method can handle complex geometries and different types of boundary conditions Therefore In this paper a Galerkin finite element method model has been developed for flow of theromohaline fliuid enclosed in an inclined shallow cavity which will be useful for many practical applications in engineering and oceanographic studies.

2. Mathematical Model and Governing Equations for a Thermohaline Fluid in an Inclined Cavity

Basic hydrodynamic equation of flow such as continuity, momentum heat transport, solute concentration and equation of state under Boussinesq approximation are

$$\frac{\partial u_j}{\partial x_j} = 0 \tag{2.1}$$

$$\left[\frac{\partial u_j}{\partial t} + u_j \frac{\partial u_j}{\partial x_j}\right] = \frac{-1}{\rho_0}\frac{\partial p}{\partial x_i} + \left[1 + \frac{\partial \rho}{\rho_0}\right] X_i + v_0 \nabla^2 u_i \tag{2.2}$$

$$\frac{\partial T}{\partial t} + S\frac{\partial T}{\partial x_j} = K_s \nabla^2 T \tag{2.3}$$

Modified Thermohaline equations are subjected to changes which follow Boussinesq variation in respect of $\rho, \mu, C_v, \alpha, \eta, k$, according to Banerjee [5] are

$$\frac{\partial u_j}{\partial x_j} \tag{2.4}$$

$$\left[\frac{\partial u_j}{\partial t} + u_j \frac{\partial u_j}{\partial x_j}\right] = \frac{-1}{\rho_0}\frac{\partial p}{\partial x_i} + \left[1 + \frac{\partial \rho}{\rho_0} + \frac{\partial \hat{\rho}}{\rho_0}\right] X_i + v_0 \nabla^2 u_i = 0 \tag{2.5}$$

$$(1 - \alpha_2 T)\left[\frac{\partial T}{\partial t} + u_j \frac{\partial T}{\partial x_j}\right] + \hat{\alpha}_2 T\left[\frac{\partial T}{\partial t} + u_j \frac{\partial T}{\partial x_j}\right] = K_T \nabla^2 T \tag{2.6}$$

$$\frac{\partial S}{\partial t} + u_j \frac{\partial S}{\partial x_j} = K_s \nabla^2 S \tag{2.7}$$

Where

$$\rho = \rho_0[1 + \alpha[T_0 - T] - \hat{\alpha}(S_0 - S)] \tag{2.8}$$

(a) Equations in a body frame

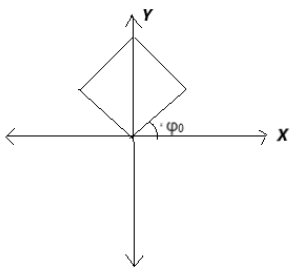

The fluid is confined in a shallow square cavity and the cavity is inclined to angle 'ϕ_0' $0 < \phi_0 < \frac{\pi}{2}$ with x-axis . The cavity is a square shallow cavity of unit length in the X-Plane making an angle ' ϕ_0 ' with X-axis. Model is defined in 2-D plane. Shallow cavity is a square from both the corner, the two directions forms the body frames and normal to it depicts the shallow depth of cavity and has been neglected in the analysis.

Transformation equations are

$$\begin{pmatrix} \hat{i} \\ \hat{j} \end{pmatrix} = \begin{pmatrix} \cos\phi_0 & \sin\phi_0 \\ -\sin\phi_0 & \sin\phi_0 \end{pmatrix} \begin{pmatrix} I \\ J \end{pmatrix}$$

Where I and J are unit vectors along x and y, $\hat{i}, \hat{j}$ are unit vectors along X' and Y'. The operators $\nabla, \nabla^2, u.\nabla$ remain invariant under this transformation.

Modified Thermohaline equation in the body turns out to be as follows:

$$\frac{\partial u}{\partial x'} + \frac{\partial v}{\partial y'} = 0 \tag{2.9}$$

$$\frac{\partial u}{\partial t} + \Big(u\frac{\partial}{\partial x'} + v\frac{\partial}{\partial x'}\Big)u = \frac{-1}{\rho_0}\frac{\partial p}{\partial x_i} - \left[1 + \frac{\partial \rho}{\rho_0} + \frac{\hat{\partial}\rho}{\rho_0}\right] g\sin\phi + v_0\nabla^2 u \tag{2.10}$$

$$\frac{\partial v}{\partial t} + \Big(u\frac{\partial}{\partial x'} + v.\frac{\partial}{\partial x'}\Big)v = \frac{-1}{\rho_0}\frac{\partial p}{\partial x_i} - \left[1 + \frac{\partial \rho}{\rho_0} + \frac{\hat{\partial}\rho}{\rho_0}\right] g\cos\phi + v_0\nabla^2 v \tag{2.11}$$

$$(1-\alpha_2 T)\left[\frac{\partial T}{\partial t} + u\frac{\partial T}{\partial x'} + V\frac{\partial T}{\partial y'}\right] + \hat{\alpha}_2 T\left[\frac{\partial S}{\partial t} + u\frac{\partial S}{\partial x'} + V\frac{\partial S}{\partial y'}\right] = K_{T_0}\nabla^2 T \tag{2.12}$$

$$\left[\frac{\partial S}{\partial t} + u\frac{\partial S}{\partial x'} + V\frac{\partial S}{\partial y'}\right] = K_{s_0}\nabla^2 S \tag{2.13}$$

Form of static solution shall remain unaltered as the state is static The variables assume the values in the new representation and are given by

$$u = 0, w = 0 \tag{2.14}$$

$$T_s = T_0 - \beta(X\sin\phi_0 + Y\cos\phi_0) \tag{2.15}$$

$$S_s = S_0 - \hat{\beta}(X\sin\phi_0 + Y\cos\phi_0) \tag{2.16}$$

$$\rho_s = \rho_0(1 + (\alpha\beta - \hat{\alpha}\hat{\beta})(X\sin\phi_0 + Y\cos\phi_0)) \tag{2.17}$$

$$P_s = P_0 - \rho_0 g[X + (\alpha\beta - \hat{\alpha}\hat{\beta})(XY\cos\phi_0 + \frac{X^2}{2}\sin\phi)]\sin\phi_0 \tag{2.18}$$

$$-\rho_0 g[X + (\alpha\beta - \hat{\alpha}\hat{\beta})\frac{Y^2}{2}\cos\phi]\cos\phi_0 \tag{2.19}$$

Perturbations over the static state are defined as

$$u_D = 0 + u^*, \qquad w_D = 0 + w^*, \rho_D = \rho s + \delta\rho^* \tag{2.20}$$

$$T_D = Ts + T^*, \qquad S_D = Ss + S^*, P_D = Ps + P^*, \qquad \delta\rho^* = -\rho_0(\alpha T^* - \hat{\alpha} S^*) \tag{2.21}$$

Since Jacobian terms and product of perturbations give rise to non-linear terms, these equations are linearized by neglecting product of perturbations and terms of order less than 10^{-2}

(b) Linearized set of equations are as follows:

(2.22)
$$u = \frac{\partial \psi}{\partial y}, v = -\frac{\partial \psi}{\partial x}$$

(2.23)
$$\frac{\partial}{\partial t}(\nabla^2 \psi) = g\alpha\left[\sin\phi_0 \frac{\partial T}{\partial y} - \cos\phi_0 \frac{\partial T}{\partial x}\right] - g\hat{\alpha}\left[\sin\phi_0 \frac{\partial S}{\partial y} - \cos\phi_0 \frac{\partial S}{\partial x}\right] + v_0 \nabla^4 \psi$$

(2.24)
$$(1-\alpha_2 T_0)\left(\frac{\partial T}{\partial t} + \beta(\cos\phi_0 \frac{\partial \psi}{\partial x} - \sin\phi_0 \frac{\partial \psi}{\partial y}\right) + \hat{\alpha_2} T_0\left(\frac{\partial S}{\partial t} + \hat{\beta}(\cos\phi_0 \frac{\partial \psi}{\partial x} - \sin\phi_0 \frac{\partial \psi}{\partial y}\right) = K_{T_0} \nabla^2 T$$

(2.25)
$$\frac{\partial S}{\partial t} + \hat{\beta}(\cos\phi_0 \frac{\partial \psi}{\partial x} - \sin\phi_0 \frac{\partial \psi}{\partial y}) = K_{S_0} \nabla^2 S$$

For the sake of brevity $*$ has been removed. As the heating is maintained at the same time invariant form, the solutions shall settle down to a steady state form.

Steady state equations are given by

$$v_0 \nabla^4 \psi = g\alpha(\cos\phi_0 \frac{\partial T}{\partial x} - \sin\phi_0 \frac{\partial T}{\partial y}) - g\hat{\alpha}(\cos\phi_0 \frac{\partial S}{\partial x} - \sin\phi_0 \frac{\partial S}{\partial y}) \tag{2.26}$$

$$[(1-\alpha_2 T_0)\beta + \hat{\alpha_2} T_0 \hat{\beta}](\cos\phi_0 \frac{\partial \psi}{\partial x} - \sin\phi_0 \frac{\partial \psi}{\partial y}) = k_0 \nabla^2 T \tag{2.27}$$

$$\hat{\beta}(\cos\phi_0 \frac{\partial \psi}{\partial x} - \sin\phi_0 \frac{\partial \psi}{\partial y}) = K_{S_0} \nabla^2 S \tag{2.28}$$

Equations are now reduced to a non-dimensional form by introducing the following scales.

$$x = x^* d, y = y^* d, \psi = \psi^* d, T = T^* \beta d, S = S^* \hat{\beta} d \tag{2.29}$$

Non-dimensional equations take the form

$$v_0\nabla^4\psi = R_T(\cos\phi_0\frac{\partial T}{\partial x} - \sin\phi_0\frac{\partial T}{\partial y}) - R_S(\cos\phi_0\frac{\partial S}{\partial x} - \sin\phi_0\frac{\partial S}{\partial y}) \tag{2.30}$$

$$\nabla^2 T = (1-\alpha_2 T_0 + R_g)(\cos\phi_0\frac{\partial\psi}{\partial x} - \sin\phi_0\frac{\partial\psi}{\partial y}) \tag{2.31}$$

$$\nabla^2 S = \frac{1}{P_S}(\cos\phi_0\frac{\partial\psi}{\partial x} - \sin\phi_0\frac{\partial\psi}{\partial y}) \tag{2.32}$$

One form of boundary conditions is

$$T(x,0) = T_0, T(x,1) = 0, S(x,0) = S_0, S(x,1) = S_1$$

$$\psi(x,0) = \psi(x,1) = \psi_x(x,0) = \psi_x(x,1) = 0$$

$$\psi(y,0) = \psi(1,y) = \psi_x(0,y) = \psi_y(1,y) = 0$$

$$T_x(x,0) = T_x(x,1) = 0$$

(c) Choice of solutions:

Closed form of the solutions satisfying the boundary conditions and equations has not feasible till date. Therefore the other approach adopted by researchers is a solution satisfying the boundary conditions but not necessarily the equations. An FEM approach has the advantage of taking care complex form of equations encompassing the geometry along with flexibility to choose solution of any degree satisfying the boundary conditions at the grids.

(d) Algorithm for Finite element method

Step 1 : Selecting global co-ordinate system for the problem under consideration

Step 2: Selecting grids along with specifications and structure of the domain as given in the problem

Step 3: Partitioning of domain into subdomains and identifying the subdomains where boundary conditions are specified.

Step 4: Mapping from global coordinate system into local coordinate system.

Step 5: Choice of Solutions and Formulation of Shape functions

Step 6. Choice of appropriate weighting functions

Step 7. Developing equation for weighted residuals

Step 8. Ensemble the weighted error equations in the whole domain

Step 9. Incorporate the boundary conditions into the system of weighted error functions.

Step 10. To set up procedure to determine solution at the nodes.

Step 11. Form the general solution in the domain using nodal solution and shape function.

Step 12.To experiment the solution identified above for analysis and behavior of the problem.

(e)Finite Element Model

(A) Mesh Generation:

The domain 'R' is sub divided into non-overlapping sub domains. Each sub domain is called as an element. Elements are connected to each other through nodes. Discretization of domain into finite element enables accurate representation of solution within each element and brings out local effects. The given domain is a square of unit length and it has been divided into smaller squares of unit length ¼.To get the accurate representation of whole domain total domain is partitioned into 16 finite elements having 25 nodes and each having four vertices each.

3. CO-ORDINATE TRANSFORMATION:

The main purpose of transforming an element from a global co-ordinate system to local co-ordinate system is for the purpose of evaluating the integral. Different elements of Mesh can be generated by assigning the global co-ordinate. The element transformation is given by

$$\xi = \frac{X - X_c}{a}, \quad \eta = \frac{Y - Y_c}{a} \tag{3.33}$$

$$\nabla^4 \psi = (R_{T1}\frac{\partial T}{\partial \xi} - R_{T2}\frac{\partial T}{\partial \eta}) - (R_{S1}\frac{\partial S}{\partial \xi} - R_{S2}\frac{\partial S}{\partial \eta}) \tag{3.34}$$

$$\nabla^2 T = (R_{g1}\frac{\partial \psi}{\partial \xi} - R_{g2}\frac{\partial \psi}{\partial \eta}) \tag{3.35}$$

$$\nabla^2 S = P_1\frac{\partial \psi}{\partial \xi} - P_2\frac{\partial \psi}{\partial \eta} \tag{3.36}$$

$$R_{T1} = R_T a^3 \cos\phi_0, \quad R_{T2} = R_T a^3 \sin\phi_0 \tag{3.37}$$

$$R_{S1} = R_S a^3 \cos\phi_0, \quad R_{S2} = R_S a^3 \sin\phi_0 \tag{3.38}$$

$$R_{g1} = R_g a^3 \cos\phi_0, \quad R_{g2} = R_g a^3 \sin\phi_0 \tag{3.39}$$

$$P_1 = \frac{1}{Ps} a\cos\phi_0, P_2 = \frac{1}{Ps} a\sin\phi_0 \tag{3.40}$$

4. Derivation of Hermite Family Finite Interpolation Function

The finite element approximation $u(x,y)$ over an element must be differentiable, linearly independent and complete. Thus the polynomial approximation is valid and is to such as to have approximate boundary conditions over a mesh and covers the range of finite values. Depending upon the requirement of the problem, approximate functions can be taken either from Lagrange family of interpolation function or then from Hermite family of interpolation function. For this particular problem, differential equations containing terms of 4^{th} order derivatives in ψ and lower order in 'T' and 'S' . Hermite interpolating polynomial containing easy accessibility for the symmetry is preferred to the Lagrange's family. We found that cubic Hermite polynomial is not sufficient to take care of higher order terms in ψ. Therefore a sixth order polynomial in two variables $\xi$and η having 16 terms has been designed. To preserve symmetry and linear independence some terms are omitted. The approximate solution over an element has been taken as

$$u^e(\xi,\eta) = a0 + a_1\xi + a_2\eta + a_3\xi^2 + a_4\xi\eta + a_5\eta^2 + a_6\xi^3 + a_7\xi^2\eta + a_8\xi\eta^2 + a_9\eta^3 + a_10\xi^3\eta + a_{11}\xi^2\eta^2 + a_{12}\xi\eta^3 + a_{13}\xi^3\eta^2 + a_{14}\xi^2\eta^3 + a_{15}\xi^3\eta^3 \tag{4.41}$$

This is the higher order minimum degree polynomial which satisfies the above condition and gives approximate shape functions. Let

$$u^e(\xi,\eta) = [X^T][a] \tag{4.42}$$

Where $X = [1,\xi,\eta,\ldots\ldots\ldots\ldots\ldots\ldots\ldots\ldots\ldots\ldots\ldots..\xi^3\eta^3]^T$

Let u_j^e denote the values of $u, u_\xi u_\eta . u_{\xi\eta}$ at the nodes. Substituting the value of ξ and η with respect to each node a_i can be determined.

$$[V^e] = [u_0, u_1, u_2, \ldots\ldots\ldots..u_{15}]^T \tag{4.43}$$

$$[V^e] = [A][a] \tag{4.44}$$

$$[a] = [A^{-1}][V] \tag{4.45}$$

D) Design of Shape Functions

$$u^e(\xi,\eta) = [X^T][a] \tag{4.46}$$

$$= [X^T][A^{-1}][V^e] \tag{4.47}$$

$$u^e(\xi,\eta) = \sum_{i=0}^{15} N_i u_i \tag{4.48}$$

Where N_i's are

$$N_i = \frac{1}{16}(1+\xi\xi_j)^2(1+\eta\eta_j)^2(2-\xi\xi_j)(2-\eta\eta_j), i = 0,1,2,3 \tag{4.49}$$

$$N_i = \frac{-\xi_j}{16}(1+\xi\xi_j)^2(1+\eta\eta_j)^2(1-\xi\xi_j)(2-\eta\eta_j), i = 4,5,6,7 \tag{4.50}$$

$$N_i = \frac{-\eta_j}{16}(1+\xi\xi_j)^2(1+\eta\eta_j)^2(2-\xi\xi_j)(1-\eta\eta_j), i = 8,9,10,11 \tag{4.51}$$

$$N_i = \frac{-\xi_j\eta_j}{16}(1+\xi\xi_j)^2(1+\eta\eta_j)^2(1-\xi\xi_j)(1-\eta\eta_j), i = 12,13,14,15 \tag{4.52}$$

The behavior of flow variable with in an element is described by shape functions, Properties of shape functions are described along with the diagram.

5. PROPERTIES OF SHAPE FUNCTIONS:

- $N_0(\xi,\eta) = N_1(\eta,\xi)$ surface is symmetric in the $\xi-\eta$ plane. Solution for 'Ψ^e', 'T^e' 'S^e' can be selected

- Extreme values occur at $(-1,-1)$
- $\frac{\partial N_0}{\partial \xi} < 0, \frac{\partial N_0}{\partial \eta} < 0 \Rightarrow$ Surface monotonically decrease with respect ξ as well η

- $N_0(1,\eta) = N_0(\xi,1) = 0$

- The surfaces N_1, N_2, N_3 behaves in a similar with the node $(-1,-1)$ in N_0 being translated to $(1,-1),(-1,1),(1,1)$ respectively.

- $N_4(-1,\eta) = N_4(1,\eta) = N_4(\xi,1) = 0$

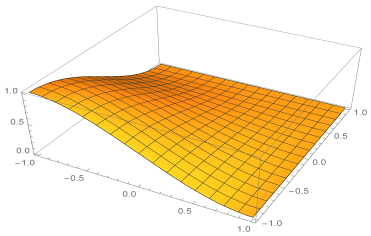

(A) SHAPE FUNCTION N0

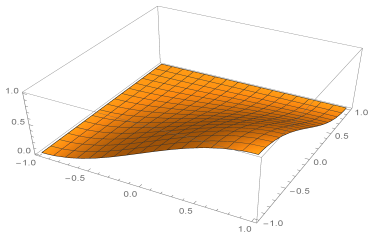

(B) SHAPE FUNCTION N1

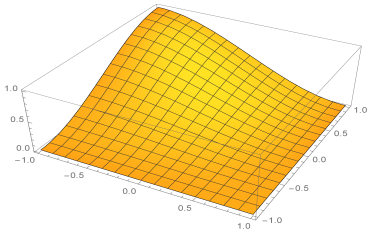

(C) SHAPE FUNCTION N2

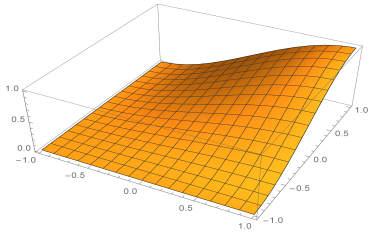

(D) SHAPE FUNCTION N3

- Local Maxima in the given domain occurs at (-0.4,-1)

- $\frac{\partial N_4}{\partial \eta} < 0 \Rightarrow$ surface is monotonically decreasing with respect to η
- Properties of $|N_5(\xi,\eta)|$, $|N_7(\xi,\eta)|$, $N_6(\xi,\eta)$ are same as $N_4(\xi,\eta)$ with the node $(-1,-1)$ in N_4 being shifted to $(1,-1),(-1,1),(1,1)$ respectively.

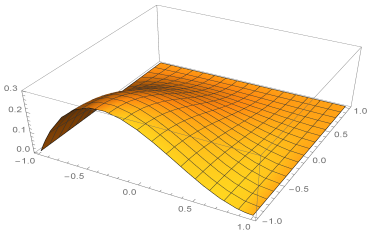

(A) SHAPE FUNCTION N4

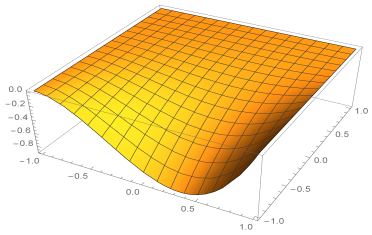

(B) SHAPE FUNCTION N5

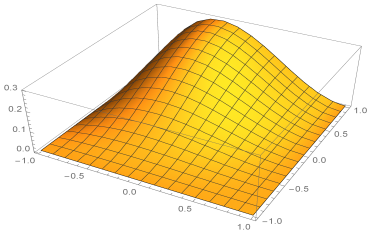

(C) SHAPE FUNCTION N6

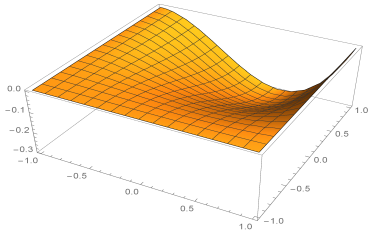

(D) SHAPE FUNCTION N7

- $N_8(\xi,-1,) = N_8(\xi,1) = N_8(1,\eta) = 0$

- $\frac{\partial N_8}{\partial \eta} < 0 \Rightarrow$ surface is monotonically decreasing with respect to ξ

- Local maxima in the given domain occurs at $(-1,-0.4)$

- Behaviour of $|N_{10}(\xi,\eta)|$, $|N_{11}(\xi,\eta)|$, $N_9(\xi,\eta)$ are same as $N_8(\xi,\eta)$ with node $(-1,-1)$ in $N_8(\xi,\eta)$ being translated to $(1,-1),(-1,1),(1,1)$ respectively.

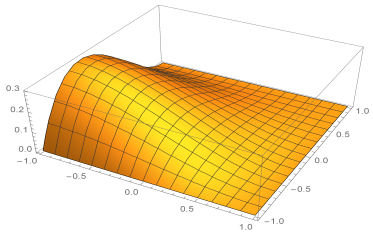

(A) SHAPE FUNCTION N8

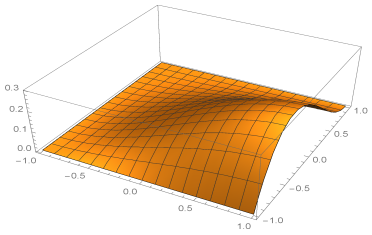

(B) SHAPE FUNCTION N9

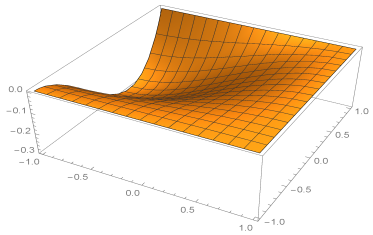

(C) SHAPE FUNCTION N10

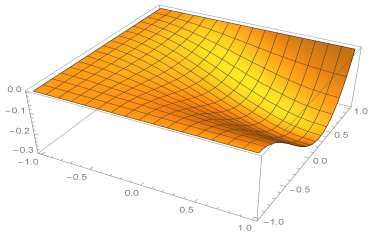

(D) SHAPE FUNCTION N11

- $N_{12}(\xi,-1,) = N_{12}(\xi,1) = N_{12}(-1,\eta) = N_12(1,\eta) = 0$

- Local maxima on the given domain occurs at $(-0.4,-0.4)$

- properties of $|N_{13}(\xi,\eta)|$, $|N_{14}(\xi,\eta)|$, $N_{15}(\xi,\eta)$ are same that of $N_{12}(\xi,\eta)$ with node $(-1,-1)$ in $N_8(\xi,\eta)$ translated to $(1,-1),(-1,1),(1,1)$ respectively.

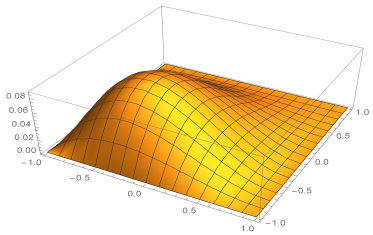

(A) SHAPE FUNCTION N12

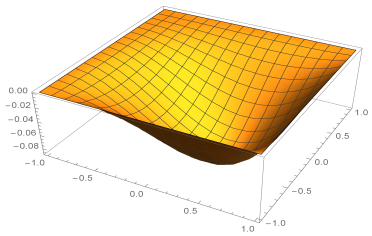

(B) SHAPE FUNCTION N13

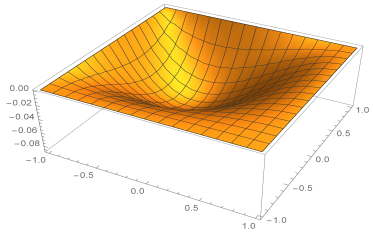

(C) SHAPE FUNCTION N14

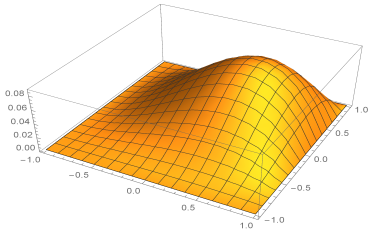

(D) SHAPE FUNCTION N15

Solution for 'ψ^e', 'T^e', 'S^e' can be selected as

$$\psi^e = [N^T, 0, 0][P] \tag{5.53}$$

$$T^e = [0, N^T, 0][P] \tag{5.54}$$

$$S = [0, 0, N^T][P] \tag{5.55}$$

$$[P^e] = [\psi_0, \psi_1, \psi_2, \ldots\ldots, \psi_{15}, T_0, T_1, \ldots\ldots\ldots\ldots T_{15}, S_0, S_1, \ldots\ldots\ldots\ldots S_{15}]^T \tag{5.56}$$

Substituting this set of solutions in the differential equation (3.41)to (3.43) the error functions are

$$E_1^e(\xi,\eta) = \nabla^4\Psi^e - R_{T1}\frac{\partial T^e}{\partial \xi} - R_{T2}\frac{\partial S^e}{\partial \eta} + R_{S1}\frac{\partial S^e}{\partial \xi} - R_{S2}\frac{\partial T^e}{\partial \eta} \tag{5.57}$$

$$E_2^e(\xi,\eta) = \nabla^2 T^e - (R_{g1}\frac{\partial \psi^e}{\partial \xi} - R_{g2}\frac{\partial \psi^e}{\partial \eta}) \tag{5.58}$$

$$E_3^e(\xi,\eta) = \nabla^2 S^e - (P_1\frac{\partial \psi^e}{\partial \xi} - P_2\frac{\partial \psi^e}{\partial \eta}) \tag{5.59}$$

The above system of expressions (5.58) to (5.60) are then represented in a simple matrix notation as

$$E^e[\xi,\eta] = [\bar{N}^e][P^e] \tag{5.60}$$

$$E^e[\xi,\eta] = [E_1^e, E_2^e, E_3^e]^T \tag{5.61}$$

$$\bar{N}^e = \begin{pmatrix} N^e_{\xi\xi\xi\xi} + 2N^{eT}_{\xi\xi\eta\eta} + N^{eT}_{\eta\eta\eta\eta} & -(R_{T1}N^{eT}_{\xi} + R_{T2}N^{eT}_{\eta}) & (R_{S1}N^{eT}_{\xi} + R_{S2}N^{eT}_{\eta}) \\ N^{eT}_{\xi\xi} + N^{eT}_{\eta\eta} & -R_{g1}N^{eT} & R_{g2}N^{eT}_{\eta} \\ N^{eT}_{\xi\xi} + N^{eT}_{\eta\eta} & -P_1 N^{eT} & P_2 N^{eT}_{\eta} \end{pmatrix}$$

Where each block is of size $16 * 16$.

The error function is now to be minimized by an appropriate method. This involves a proper choice of weighted residuals. Here it may be noted that nature of the solution plays dominant role over the nature of error function. Hence weighted function proportional to solution is the appropriate choice for the solution. This gives Galerkin method of error analysis.

E Weighted Residual using Galerkin Method

$$< W, E >= \int_D W.E dx = 0 \tag{5.62}$$

In Galerkin method weighting function is chosen to be $W_j = \frac{\partial u}{\partial N_i}$ where $u = \sum_{e=1}^{16} N_i^e u_i^e$ is the approximate solution for the problem of an element 'e'. Minimization process in Galerkin method for the above solution is

$$\int_{-1}^{1}\int_{-1}^{1} N_j E_k^e(\xi,\eta) d\xi d\eta = 0, i = 0, 1, ...15 \tag{5.63}$$

This can be written in the matrix form as

$$[W^e] = [M^e][P^e] \tag{5.64}$$

Where $[W^e] = [W_{1j^e}, W_{2j^e}, W_{3j^e}]^T$ is a column matrix of size $48 * 1, j = 0, 1, .., 15$

$[M^e] = \begin{pmatrix} M_{11} & M_{12} & M_{13} \\ M_{21} & M_{22} & M_{23} \\ M_{31} & M_{32} & M_{33} \end{pmatrix}$ where each block is of size 16x16.

$[P^e]$ represents a column matrix of 48 elements taking '12'nodal values for each node taken anticlockwise. They are numbered as

$$[P^e] = [\psi_0, \psi_1, \psi_2, \psi_3, \psi_{\xi 0}, \psi_{\xi 1}, \psi_{\xi 2}, \psi_{\xi 3} \ldots\ldots,]^T \tag{5.65}$$

(72) The coefficient matrix $[M^e]$ is same for all elements. Assembly of elements is based on the idea that coefficients coming from all elements connected at one node will add up and solutions are continuous at the boundaries.

Equivalence relation at the nodes is given as follows.

For $i \neq 0, i \neq 4$

$$\psi_{i,j}^{4(j-1)+(i-1)} = \psi_{i,j}^{4(j-1)+i} = \psi_{i,j}^{4j+4(i-1)} = \psi_{i,j}^{4j+i} \tag{5.66}$$

For $i = 0$

$$\psi_{i,j}^{4(j-1)+i} = \psi_{i,j}^{4j+i} \tag{5.67}$$

For $i = 4$

$$\psi_{i,j}^{4(j-1)+4(i-1)} = \psi_{i,j}^{4j+(i-1)} \tag{5.68}$$

Each element is identified as the position $4j+I$ and nodes as $5j+i, j = 0,1,2,3$ The system of equations (5.64) is augmented over the region as follows.

6. Derivation of Domain Equation $AX = 0$

The system of equation is reconstructed as follows. The set of 48 elements $[P^e]$ has been recasted as $[\psi_0, \psi_{\xi 0}, \psi_{\eta 0}, \psi_{\xi \eta 0}, \ldots\ldots\ldots\ldots..]$.This reindexing has been used to rearrange the elements. A relation connecting an element and its four nodes are given in (5.65) and this is used to augment the equation over the whole domain to give us total weighted error over the region. All the elements and nodes of the region are continuously numbered from 0to 15 and 0to 24 respectively.

The transformation $[P^e]$ to $[\bar{P}]$ is the mapping $P : K = (5l+i)*12$. Corresponding to the matrix $[M^e]$ has been transformed to $[\bar{M}]$ by the following rule. $M_{ij} \rightarrow M_{(5l+M)*12.(5l+M)*12}, \quad l = 0,1,2,3,4, m = 0,1,2,3,4$ This mapping has been carried out for all 'e' over the whole region and it is given as

$$\bar{m} = \sum_{e=1}^{16} M_{ij}^e$$

Thus the system is transformed to $AX = 0$ where A is a matrix of size $300*300$ and 'X' is a column matrix of size $300*1$ respectively.

6.1. Design of the matrix $AX = B$ resulting from boundary conditions. Firstly we identified the nodes where boundary conditions are prescribed. Inserting this 'm' nodal values in $AX = 0$, the size of the coefficient matrix and solution matrix reduces to $nn - m$ and $n - m1$ respectively. This is an over specified set of equations. For a consistent system unique solution exists when rank of coefficient matrix is equal to number of unknowns. Several approaches have been given in the literature to obtain unique solution of the equation. Two obvious approaches are (1) reduction of the equations $AX = 0$ to an $(n-m)(n-m)$ form, forming the equation $AX = B$.(2)Augmenting the equation AX=0 to AX=B by appropriately re-defining A and B. The second approach is known as Wilson's approach. Here we are using the lateral approach to obtain the nodal solutions in the problem if $X_j = \upsilon_j$, $j = 1,2,\ldots..m$ is prescribed at nodal points.

The A and B matrices are transformed as follows. The column j of $[a_{ij}]$ is multiplied by υ_j and this column is added to [B]. This procedure is repeated for every 'i' of prescribed boundary. This reformulated matrix is restructured by replacing every row-element of [B] by υ_i for every 'i'. At the same time, all the elements of ith row and i th column are replaced by zero and aii has been repeated for every 'i'. This procedure has been repeated for every 'i' where boundary conditions are prescribed. This non-homogeneous set of equations are solved by standard routine. Based on the algorithm, software may be developed to understand large scale phenomena related cavity flows of thermohaline fluids.

CONCLUSION AND FUTURE SCOPE

In this paper a computational model for flow of thermohaline fluid enclosed in a shallow cavity using Galerkin Finite element method has been developed. This model can be extended to various cavity flows related to thermohaline flows occurring in various applications subjected to appropriate boundary conditions ranging from industrial problems to oceanic flows This work may be extended to cavities consisting of complex geometries in real time studies.

CONFLICT OF INTERESTS

The author(s) declare that there is no conflict of interests.

REFERENCES

[1] A.E. Gill, The boundary layer regime for convection in a rectangular cavity. J. Fluid Mech. 26 (1966), 515-536.

[2] J.P. Garandet, T. Alboussiere, R. Moreau, Buoyancy driven convection in a rectangular enclosure with a transverse magnetic field, Int. J. Heat Mass Transfer. 35 (1992), 741–748.

[3] H. Ozoe, K. Okada, The effect of the direction of the external magnetic field on the three-dimensional natural convection in a cubical enclosure, Int. J. Heat Mass Transfer. 32 (1989), 1939–1954.

[4] P. Vasseur, M. Hasnaoui, E. Bilgen, L. Robillard, Natural Convection in an Inclined Fluid Layer With a Transverse Magnetic Field: Analogy With a Porous Medium, J. Heat Transfer. 117 (1995), 121–129.

[5] M.B. Banerjee, J.R. Gupta, J. Prakash, On Thermohaline Convection of the Veronis Type, J. Math. Anal. Appl. 179 (1993), 327–334.

[6] J.A. Whitehead, Abrupt Transitions and Hysteresis in Thermohaline Laboratory Models, J. Phys. Oceanogr. 39 (2009) 1231–1243.

[7] R. Menon, Flow analysis of thermohaline fluid periodically heated from below. Int. J. Pure Appl. Math. 118 (2018), 873-882.

[8] R. Menon, A. Kulkarni, M. Venkatesan, Stability Analysis of a non-autonomous system of thermo haline convection heated periodically from below. J. Adv. Res. Dyn. Control Syst. 10 (2018), 1608-1614.